Published in final edited form as:
Acta Neuropathol. 2014 June ; 127(6): 897–909. doi:10.1007/s00401-014-1272-4.

Human Pontine Glioma Cells Can Induce Murine Tumors

Viola Caretti[1,5,6,7,*], **A. Charlotte P. Sewing**[5,6,7], **Tonny Lagerweij**[5,6,7], **Pepijn Schellen**[5,6,7], **Marianna Bugiani**[8], **Marc H. A. Jansen**[5,7], **Dannis G. van Vuurden**[5,7], **Anna C. Navis**[10], **Ilona Horsman**[9], **W. Peter Vandertop**[6], **David P. Noske**[6,7], **Pieter Wesseling**[7,8,10], **Gertjan J.L. Kaspers**[5], **Javad Nazarian**[3], **Hannes Vogel**[2], **Esther Hulleman**[*,5,6,7,#], **Michelle Monje**[1,*,#], and **Thomas Wurdinger**[4,6,7,*,#]

[1]Departments of Neurology, Neurosurgery and Pediatrics, Stanford University School of Medicine, Stanford [2]Department of Pathology, Stanford [3]Research Center for Genetic Medicine, Children's National Medical Center, Washington, United States [4]Department of Neurology, Massachusetts General Hospital and Harvard Medical School, Boston, Massachusetts, United States [5]Department of Pediatric Oncology, VU University Medical Center, Amsterdam [6]Department of Neurosurgery, VU University Medical Center, Amsterdam [7]Neuro-oncology Research Group, VU University Medical Center, Amsterdam [8]Department of Pathology, VU University Medical Center, Amsterdam [9]Department of Clinical Genetics, VU University Medical Center, Amsterdam [10]Department of Pathology, Radboud University Medical Centre, Nijmegen, The Netherlands

Abstract

Diffuse intrinsic pontine glioma (DIPG), with a median survival of only nine months, is the leading cause of pediatric brain cancer mortality. Dearth of tumor tissue for research has limited progress in this disease until recently. New experimental models for DIPG research are now emerging.

To develop preclinical models of DIPG, two different methods were adopted: cells obtained at autopsy 1) were directly xenografted orthotopically into the pons of immunodeficient mice without an intervening cell culture step or 2) were first cultured *in vitro* and, upon successful expansion, injected *in vivo*. Both strategies resulted in pontine tumors histopathologically similar to the original human DIPG tumors. However, following the direct transplantation method all tumors proved to be composed of murine and not of human cells. This is in contrast to the indirect method that included initial *in vitro* culture and resulted in xenografts comprised of human cells. Of note, direct injection of cells obtained *post mortem* from the pons and frontal lobe of human brains not affected by cancer did not give rise to neoplasms. The murine pontine tumors exhibited an immunophenotype similar to human DIPG, but were also positive for microglia/macrophage

Correspondence to: Viola Caretti & Michelle Monje, 265 Campus Drive, Room G3077, Stanford, CA 94305, +1 (650) 721-5750. vcaretti@stanford.edu & mmonje@stanford.edu. Thomas Wurdinger & Esther Hulleman, VU University Medical Center, CCA Room 3.34, De Boelelaan 1117, 1081 HV Amsterdam, The Netherlands. Phone: +31-(0)204447909. t.wurdinger@vumc.nl & e.hulleman@vumc.nl.
*Co-corresponding authors
#These authors contributed equally

Conflict of interest: none declared

markers, such as CD45, CD68 and CD11b. Serial orthotopic injection of these murine cells results in lethal tumors in recipient mice.

Direct injection of human DIPG cells *in vivo* can give rise to malignant murine tumors. This represents an important caveat for xenotransplantation models of DIPG. In contrast, an initial *in vitro* culture step can allow establishment of human orthotopic xenografts. The mechanism underlying this phenomenon observed with direct xenotransplantation remains an open question.

Keywords

Neoplasms; Pontine Neoplasms; Animal Disease Model; Microglia

Introduction

Diffuse intrinsic pontine glioma (DIPG) is a devastating brain cancer affecting mainly children [19,22]. Compared to other brain malignancies, DIPG carries the worst prognosis; the majority of affected children die within one year from diagnosis [10,12]. DIPG is also one of the pediatric tumors that has been the least investigated in laboratories, due to a lack of primary tissue available for research and the paucity of robust preclinical models. We have established autopsy protocols to develop experimental models of DIPG and to investigate its biology [7,30].

Recent studies have shown that DIPG is molecularly distinct from adult high-grade gliomas [35,49]. Although DIPG shares recurrent aberrations in histone 3 genes with supratentorial pediatric gliomas, they are molecularly distinct tumors [42,43,49]. DIPG is characterized by unique hallmarks including a remarkable spatiotemporal specificity (occurring in the ventral pons during mid-childhood) and a diffuse growth pattern. As the disease progresses, DIPG often invades the cerebellum and even supratentorial brain regions, such as the thalamus, lateral ventricles and cerebral cortex [54]. DIPG infiltrative growth and the delicate anatomical location where it arises preclude surgical resection. The pontine microenvironment at mid-childhood may be of paramount importance in the biology, pathogenesis and infiltrative nature of DIPG [6,30]. To find a cure for this disease, it is critical to identify the microenvironmental and genetic factors that allow the tumor to spread throughout the brainstem and the entire brain.

Here, we present data showing that direct injection of human DIPG cells obtained from *post mortem* tissue produced tumors composed exclusively of murine cells, while injection of human DIPG cells, obtained at autopsy but first cultured *in vitro,* gave rise to human xenografts. In comparison, direct injection of cells obtained *post mortem* from the pons and frontal lobe of human brains not affected by cancer did not give rise to murine neoplasms. The cells of these induced murine neoplasms exhibited immunocytochemical markers consistent with DIPG and also with the microglia/macrophage phenotype.

Materials and Methods

Tissue Donors

All tumor samples were post-treatment autopsy specimens from VU University Medical Center Amsterdam (VUMC) (The Netherlands), Stanford University (SU) and Children's National Medical Center (CNMC) in Washington DC (United States). Patients were included if they had classic DIPG MRI findings and clinical presentation. All parents signed informed consent forms for the use of biological material after autopsy for research purposes; and the appropriate Institutional Review Board (IRB) approved all procedures. The autopsy protocols have been previously reported [7,30]. Patients' clinical characteristics are summarized in Table 1 and in Supplementary Table 1. For clarity, the suffix "h" for human and "m" for murine will be used in front all patients and cell lines and tumor sample names. All human patients affected by DIPG were treated with radiotherapy and/or chemotherapy, with the exception of patient h-SU-DIPG-I, who received only minimal treatment for the tumor [30].

The human donor brains used for control tissue were obtained from the National Development and Research Institute (NDRI) (http://www.ndri.org). The donors were males not affected by brain cancer; they were age 53 (cause of death: cardiac arrest) and age 59 (cause of death: respiratory disease); the samples collected were named h-SU-NDRI-2 and h-SU-NDRI-3, respectively. The death-autopsy interval was 12.5 hours for h-SU-NDRI-2 and 5.56 hours for h-SU-NDRI-3.

Direct and Indirect Xenotransplantation Methods

For the direct transplantation method, immediately after rapid brain autopsy of four DIPG patients (h-VU-DIPG-3, -4 and -5 and h-CNMC-D1; mean *post mortem* delay was 3.4 hours) [7], a single cell suspension was prepared from pontine tissue macroscopically infiltrated by tumor. Tumor material was cut in 0.5 cm^3 pieces with a sterile scalpel and mechanically dissociated using a 100μm strainer and resuspended in Optimem medium or, for injection subcutaneously, in Matrigel (BD biosciences) diluted 1:3 in phosphate buffered saline (PBS).

The indirect method, previously described [30], also followed rapid brain autopsy of DIPG patients (h-SU-DIPG-VI; *post mortem* delay was 2 hours). Briefly, for chemical dissociation, minced tissue was placed in Hepes-HBSS with DNaseI (250 U/mL) and collagenase type IV (1 mg/mL) at 37°C on a Nutator (Fisher Scientific). Cells were then further mechanically dissociated using 100, 70 and 40 μm strainers in series. Next, a 30% sucrose gradient and the ACK lysis buffer (Invitrogen) were employed to deplete myelin and red blood cells, respectively. Finally, the single cells suspension was cultured in serum-free Tumor Stem Media (TSM) consisting of Neurobasal media (-A) (Invitrogen), B27 (-A) (Invitrogen), human-basic FGF (20 ng/mL; Shenandoah Biotech), human EGF (20 ng/mL; Shenandoah Biotech), human PDGF-AA and -BB (20 ng/mL; Shenandoah Biotech), and heparin (10 ng/mL) [30].

Primary Tumor Cell Culture

Human SU-DIPG-VI cells were cultured in TSM, as described above. After extraction from subcutaneous tumors (m-VU-DIPG-3 and -5) and from pons xenograft (CNMC-D1 cells), murine cells were cultured in NeuroCult Basal Medium (StemCell Technologies) supplemented with murine EGF (20 ng/mL; Shenandoah Biotech), murine FGF (20 ng/mL; Shenandoah Biotech) and heparin (10 ng/mL).

Stereotactic DIPG Cell Injection

All animal experiments were approved and performed according to the guidelines of the VU University Ethical and Scientific Committee on Animal Experiments, of Stanford University Institutional Care and Use Committee and of CNMC Institutional Animal Use and Care Protocols (#01429, #01335).

At the VU non-obese diabetic (NOD)–severe combined immunodeficiency (SCID) mice and female athymic nude (age six–twelve weeks; Harlan), at Stanford NOD-SCID-IL2 gamma chain deficient (NSG) mice (age P1–5 and six–twelve weeks; The Jackson Laboratory) and at the CNMC nude mice J:NU (age P-5, The Jackson Laboratory) were kept under specific pathogen-free conditions in air-filtered cages and received food and water *ad libitum.* We have previously reported the procedures used for stereotactic tumor cell transplantation both in adult [8] and in pups [30] mice and for tumor cell injection subcutaneously [8]. For surgeries in adult mice, 1×10^6 human DIPG cells/5μL or 1×10^5 murine VU-DIPG-3 and -5 cells/5μL were injected in the pons or striatum of immunodeficient mice. For adult mice, the stereotactic coordinates used to target the pons were: 0.8 mm posterior to lambda, 1 mm lateral to the sagittal suture and 5 mm deep; and to target the striatum were: 2 mm anterior to bregma, 0.5 mm lateral to the sagittal suture and 2 mm deep. For pup surgeries, 4×10^4 cells/5μL were injected in the IV^{th} ventricle, using the following coordinates: 3 mm posterior to lambda, 0 mm lateral to the sagittal suture and 3mm deep.

Immunohistochemical Staining

Immunohistochemistry (IHC), immunofluorescence (IF), and fluorescence *in situ* hybridization (FISH), were performed on 5 μm tissue sections of paraffin-embedded (IHC and FISH) or fresh frozen (IF) human and murine DIPG tumor samples. IHC was performed as previously described [7]. The following antibodies were used: NeuN (mouse monoclonal, 1:1,600, Millipore), GFAP (rabbit polyclonal, 1:300, Dako), Synaptophysin (mouse monoclonal, 1:150, Dako), CD45 (mouse monoclonal, 1:1000, Dako), CD3 (rabbit polyclonal, 1:100, Cell Marque), CD68 (monoclonal mouse, 1:1600, Dako) and CD163 (mouse monoclonal, 1:50, Novocastra) all against human and mouse antigen; Vimentin (mouse monoclonal, 1:4000, Dako) and Ki67 (mouse monoclonal, 1:160, Dako) specifically reacting with the human antigen; Ki67 (rabbit polyclonal, 1:2,000, Dianova) specifically reacting with the mouse antigen. Antigen retrieval was performed by microwave heating, in citrate buffer (pH 6) for Glut-1, Vimentin and GFAP antibodies and in TRIS-EDTA (pH 9) for NeuN and Ki67 antibodies, while Synaptophysin-staining required no antigen retrieval. For CD45, CD3 and CD163, Ventana's proprietary antigen retrieval solution (pH 8.5), and, for CD68, Leica's proprietary antigen retrieval solution (pH 6.0) were used. All antibodies were incubated for one hour at room temperature Powervision (Glut-1, Ki67, NeuN and

Synapthophysin) and Envision (Vimentin, GFAP) were used for visualization (both from Dako). Visualization for CD3, CD68, CD45, and CD163 was performed by the Ventana iVIEW DAB Detection Kit. IF was carried out as described in a previously published protocol [4] with the exception that antibody incubation time was 24 hours. Additional antibodies used not reported in [4] were: SOX2 antibody (rabbit polyclonal, 1:200, Millipore) and Human Nuclei (mouse monoclonal, 1:200, Millipore). FISH was performed as previously reported [38]. The chromosome enumeration probe 1 (CEP1 Spectrum Orange Probe, diluted 1:10 in uni-44 buffer, Abbott Molecular, Abbott Park, Illinois, USA) was used. Hybridization was performed overnight at 37°C.

Karyotyping

Metaphase preparations of m-VU-DIPG-3 and -5, m-CNMC-D1 and h-SU-DIPG-VI cells were obtained by standard cytogenetic procedures of mitotic arrest, hypotonic shock and cell fixation. Metaphase cells were stained by standard G-banding methodology and imaged using a Zeiss Axioskop 20 microscope with 100x plan apochromatic objective and a CytoVision imaging system (Leica Microsystems, USA).

Array-Comparative Genomic Hybridization and Sanger Sequencing of Exons

Human VU-DIPG-3 and -5 somatic tumor DNA was isolated from the original pontine tumor. Non-somatic DNA was isolated from areas far away from the original pontine tumor (temporal lobe) with no macroscopic signs of intraparenchymal tumor growth. Cases were independently reviewed by a senior neuropathologist (PW) according to the World Health Organization (WHO) guidelines. Histologically, both tumors were labeled as glioblastoma (GBM) (Table 1). Control murine DNA was isolated from corresponding nude or SCID mice. DNA was isolated from fresh-frozen tissue using an all prep DNA/RNA isolation kit (Qiagen).

Samples were labeled and hybridized on human and murine Array-Comparative Genomic Hybridization (aCGH) oligo Microarray 4×180k (Agilent Technologies, Palo Alto, CA), as previously described [24]. Image acquisition of the Agilent arrays was performed using the Agilent DNA Microarray scanner G2505C, and image analysis was performed using Feature Extraction software version 10.5.1.1 (Agilent Technologies). Amplifications of EGFR, PTEN and PDGFR-α were analyzed by verifying intensity of hybridized probes in the genomic regions of these genes.

Exons coding of interest on H3F3A, HIST1H3B and PI3KCA (H1047R/L and E542K) were sequenced using Sanger fluorescent sequencing after amplification by polymerase chain reaction using standard methods. The primers were designed using primer BLAST from NCBI (Supplementary Table 2). PCR products were directly sequenced using BigDye® Terminator v3.1 Cycle Sequencing Kit (Life technologies) and analyzed by a genetic analyzer (Applied Biosystems).

DNA Fingerprinting

Short tandem repeat (STR) analysis was performed according to the manufacturer protocol (PowerPLex 18D system, Promega). The STR fingerprint for h-SU-DIPG-VI control cortex is reported in Supplementary Table 3.

Flow Cytometry

After *in vitro* culture, h-SU-DIPG-VI and m-CNMC-D1 cells were enzymatically dissociated as previously described [30], subcutaneous m-VU-DIPG-3 and -5 tumors were mechanically dissociated as described above. The following antibodies were incubated for one hour: PerCP-Cy5.5 anti-mouse H-2K^{d}, PE anti-human HLA-A,B,C, Brilliant Violet421™ anti-mouse CD45 (all by BioLegend) and PE-Cyanine7 anti-mouse and human CD11b (eBioscience). Cells were gated on the basis of forward- and side-scatter profiles, and live/dead discrimination was obtained with 7-amino-actinomycin D (7-AAD) (DAPI) or Propidium Iodide. Flow cytometry was performed using a FACS Aria II (BD Biosciences). Data were analyzed with FlowJo software.

Results

DIPG xenografts resemble the original human neoplasm histologically

To establish xenograft DIPG models, we used early *post mortem* autopsy protocols at the VU [7] and at Stanford University School of Medicine [30]. While at the VU a direct transplantation strategy was adopted, at Stanford human DIPG cells were first cultured *in vitro* and subsequently, upon successful expansion, injected *in vivo* (indirect method) (Fig. 1a). In the direct transplantation method, *post mortem* DIPG tissue (h-VU-DIPG-3, -4 and -5) was immediately dissociated using rapid mechanical mincing and straining, without chemical processing of the sample or myelin depletion. The single cell suspension was directly injected subcutaneously (10×10^{6} cells/100 μl/flank) and into the brain (pons and striatum; 1×10^{6} cells/5 μl) of immunodeficient mice (n=3/patient) (Fig. 1a, left panel). In the indirect method, *post mortem* DIPG tissue (h-SU-DIPG-VI) was dissociated enzymatically and the single cell suspension was cultured and expanded *in vitro.* Once neurospheres formed and expanded *in vitro,* cells were enzymatically dissociated and injected in the pons of NSG pups (Fig. 1a, right panel).

Neither the direct or indirect method resulted in subcutaneous tumor growth. Mice that received direct cell injection into the pons were sacrificed due to neurological symptoms after three, six, and nine months for the h-VU-DIPG-5, -3 and -4 xenografts, respectively. Necropsy analysis showed that human DIPG cells, injected directly into the pons, gave rise to tumors in 3 out of 3 autopsy cases (transplant generation 1); only for one autopsy case, h-VU-DIPG-3, tumor developed in the striatum (transplant generation 1). Human SU-DIPG-VI xenografts produced neurological symptoms after approximately six months.

Histologically, all tumors showed characteristics of the original human DIPG tissue including the diffuse growth pattern, hallmark of DIPG (Fig. 1b and Supplementary Fig. 1a–j). Human DIPG tumors are highly heterogeneous [5,34], m-VU-DIPG-3 and -5 resembled the small-cell component observed in the corresponding h-VU-DIPG-3 and -5 tumors (Fig.

1c and Supplementary Fig. 1). Human VU-DIPG-3 and -5 presented perivascular growth, as did m-VU-DIPG-3 and -5 (Supplementary Fig. 1b, d, f, g and l). Leptomeningeal spread in human DIPG is often detected at recurrence [44] and it was found both in h-VUMC-DIPG-5 and in m-VU-DIPG-3 and -5 (Fig. 1b and Supplementary Fig. 1c, f, and i). Perineuronal satellistosis [30] was also found both in the h-VUMC-DIPG-3 and -5 and in the m-VUMC-DIPG-3 and -5 (Supplementary Fig. 1h). Tumor invasion in the skull bone was found after direct xenotransplantation of h-VU-DIPG-5 cells in the murine pons (Supplementary Fig. 1k). Of note, after the m-VU-DIPG-3 and -5 were transplanted subcutaneously and thereafter in the murine pons, along with the diffuse tumor spread, areas of more compact growth were also detected (Supplementary Fig. 1g).

To establish VU-DIPG-3, -4 and -5 mouse models and given the low *in vitro* proliferation rate of VU-DIPG-3, -4 and -5 cells, serial tumor transplantations was performed. Once mice showed neurological symptoms, brain were harvested and affected areas were resected using sterile instruments. A single cell suspension was prepared (mechanical dissociation), and cells were re-injected into the pons of nude mice (transplant generation 2; n=3) and subcutaneously in Matrigel (n=2). This time, tumors developed both subcutaneously and in the pons for m-VU-DIPG-3 and m-VU-DIPG-5 within three weeks post-injection (Fig. 1a, left panel), while no tumor growth could be detected for m-VU-DIPG-4 nine months post-injection. Via serial transplantation in nude mice the m-VU-DIPG-3 and -5 models were established. For subsequent experiments, m-VU-DIPG-3 and -5 cells were first expanded subcutaneously and thereafter injected in the murine pons (transplant generations 3–10).

Direct injection of human DIPG cells in the murine pons gives rise to murine tumors

The tumors that developed after direct injection of h-VU-DIPG-3, -4 and -5 cells into the murine pons were comprised of murine instead of human cells (Fig. 2a–d and g). Conversely, h-SU-DIPG-VI cells injected in the pons after *in vitro* passaging gave rise to human tumors (Fig. 2e and f).

Several lines of evidence were used to verify that the m-VU-DIPG-3 and -5 tumors were entirely composed of murine cells. For the purpose of comparison, we used tissue of the h-E98-FM adult glioblastoma-derived pontine xenografts, known to be of human origin [8]. The exclusive presence in the normal murine karyotype of telocentric chromosomes is a major morphologic distinction from the human karyotype, which has no true telocentric chromosomes. Additionally, mouse and human chromosomes are readily separable by their distinct G-band patterns and their normal diploid number, 40 and 46, respectively. Analysis of m-VU-DIPG-3, -5 and m-CNMC-D1 cells demonstrated only chromosomes of obvious murine origin by telocentric morphology and banding pattern. No human chromosomes were observed. Conversely, h-SU-DIPG-VI demonstrated human chromosomes only, as assessed by morphology and banding pattern (Fig. 2b and Supplementary Fig. 2). The modal chromosome count for m-VU-DIPG-3 was 41 (range: 40–44). Murine VU-DIPG-5 demonstrated cells of 40 and 80 (tetraploid) chromosomes. Murine CNMC-D1 demonstrated bimodal populations of 40 chromosomes (range 39–40) and 81 (range 56–81). Human SU-DIPG-VI demonstrated an average 95 chromosomes (range: 84–112, near-tetraploid).

Next, we performed IHC employing antibodies raised against specific human or murine antigens. First, m-VU-DIPG-3 and -5 tumors were negative for human Vimentin, in contrast to h-E98-FM tumor tissue (Fig. 2c). Second, Ki67 antibodies directed specifically against the human antigen did not react in the m-VU-DIPG-3 and -5 tissues, whereas Ki67 directed against the mouse antigen did react, again in contrast to h-E98-FM tumor tissues (Fig. 2d).

Further, cross species hybridization of m-VU-DIPG-3 and h-VU-DIPG-3 on both human and murine aCGH platforms led to a clear decrease in the amount of DNA hybridization on the arrays of the opposite species (Supplementary Fig. 3) and neither platforms showed an analyzable profile, suggesting no large somatic human sequences were retained in the murine tumor. After correction for species-specific location of alleles on the genome, hybridization of m-VU-DIPG-3 DNA on the proper platform showed no corresponding gains and losses between mouse and human tumors (Table 2). In addition, via exon sequencing the presence of known DIPG mutations and amplifications was analyzed both in the human and murine tumors. The only aberration detected in the human VU-DIPG-3 and 5 (H3F3A K27M) was not present in the corresponding murine tumors (Table 2).

Human SU-DIPG-VI xenograft tissue revealed Human Nuclei staining and human Vimentin staining (Fig. 2e and f, upper panels). When analyzed by flow cytometry, h-SU-DIPG-VI cells cultured *in vitro* only exhibited, as expected, 99% positivity to HLA (marker for the human major histocompatibility complex) and no cell positivity for H-2K^{d} (marker for the murine major histocompatibility complex in the immunodeficient mice strains used in this study) (Fig. 3e, right panels). These data indicate that human DIPG cells, when first cultured *in vitro*, engraft in the murine brain and give rise to tumors of human origin. The h-SU-DIPG-VI cells as well as the h-SU-DIPG-VI xenograft harbored the H3F3A K27M mutation (Table 1).

Development of murine neoplasms using the direct transplantation method was observed independently at two institutions (at the VUMC and at the CNMC). At the CNMC, human DIPG cells gave rise to a murine tumor, named m-CNMC-D1. Murine CNMC-D1 cells were negative both for Human Nuclei and human Vimentin staining (Fig. 2e and f, lower panels). DNA fingerprinting was performed on DNA obtained from m-VU-DIPG-3, -5, m-CNMC-D1, h-SU-DIPG-VI cells, and from a tail biopsy of an NSG mouse (m-DNA-CTRL). On the gel, human STR are identified by bands lower than 500 base pairs (bp); while h-SU-DIPG-VI and h-DNA-CTRL showed a clear band pattern lower than 500 bp, no bands lower than 500 bp was identified for any of the murine samples (Fig. 2g). Next, m-VU-DIPG-3, -5 and m-CNMC-D1 cells were analyzed by flow cytometry; no HLA positive cells could be detected, while 93%, 94% and 12% of the cells resulted positive to H-2K^{d}, respectively (Fig. 3e, left and central panels).

To test if this phenomenon could have been caused by cells derived from apparently normal human brain tissue rather than from tissue affected by DIPG, we collected *post mortem* samples from the pons and frontal lobe of two patients not affected by brain cancer. We used the exact same extraction, tissue dissociation and direct transplantation method employed for human DIPG tissue. NSG mice were injected subcutaneously or in the pons or in the frontal lobe with human noncancerous brain cells or with PBS. After 6 to 9 months mice did

not show any subcutaneous mass, weight loss or neurological symptoms, therefore mice were sacrificed and the brains analyzed. No tumor was detected in tissue slices stained with hematoxylin and eosin (H&E) (data not shown). Staining for Ki67 did not show any proliferation with the exception of cells lining the needle trajectory (Fig. 2h).

Taken together, these data indicate that human DIPG cells derived from tissue collected at autopsy and injected directly into the pons of immunodeficient mice, but not after *in vitro* passaging, induce lethal murine brain tumors.

Murine tumors are positive both for immunomarkers seen in DIPG and for microglia/macrophage markers

We then set out to characterize the cell identity of these pontine murine tumors. By analyzing both human and murine healthy pontine tissue at different ages, our group previously identified a specific cell population present uniquely in the ventral pons and at mid-childhood (corresponding to P21 in mice). Hence, these cells, defined as pontine precursor-like cell (PPC), could be the cells of origin of DIPG [30]. PPCs express Nestin, Olig2 and SOX2 but not GFAP [30]. The DIPG immunophenotype is very similar, but typically exhibits GFAP immunopositivity [30]. Interestingly, the murine pontine tumors also revealed the $Nestin^{+}/Olig2^{+}/SOX2^{+}/GFAP^{-}$ phenotype [30] (Fig. 3a). The m-VU-DIPG-3 and -5 tumors did not exhibit NeuN/Synaptophysin immunopositivity, arguing against a neuronal origin of these neoplasms (Fig. 3b). Consistent with previous reports [30,54] the h-VU-DIPG-3 and -5 primary tumor, while exhibiting cells that are $Nestin^{+}/Olig2^{+}$, also exhibited a high percentage of $GFAP^{+}$ cells (Fig. 3c).

Intriguingly, almost all m-VU-DIPG-3 and -5 cells were CD68+ and CD45+, as detected by IHC (Fig. 3d) and flow cytometry analysis (Fig. 3e, left panel). In addition, approximately 7% of the m-VU-DIPG-3 and -5 cell population resulted positive for CD11b (Fig. 3e, left panel), indicating that these cells not only exhibit an immunophenotype characteristic of neural precursor cells but also characteristic of microglia/macrophages [40]. Next, we tested m-CNMC-D1 cells and h-SU-DIPG-VI cells for the presence of microglia/macrophage markers, and, while both were negative for CD45, they did present a subpopulation of cells positive for CD11b, 16% and 19%, respectively (Fig. 3e central and right panel). In line with this evidence, h-SU-DIPG-VI xenografts exhibited cells positive both for Human Nuclei antibody and CD68 (Fig. 3d, right panel). Finally, we stained six human DIPG *post mortem* tissue samples (Supplementary Table 1) for CD45 (marker for inflammatory cells), CD68 and CD163 (marker for microglia/macrophages) and CD3 (marker for T-cells). While only few cells were positive for CD45 and CD3, a significant number of CD68 and CD163 positive cells were found within the tumor parenchyma (Fig. 3f).

Discussion

DIPG, with a two-year overall survival rate less than 2%, is the pediatric brain malignancy with the worst prognosis. In the last thirty years, significant improvement in survival has been achieved in other pediatric cancers, while no progress has been made for children affected by DIPG, despite numerous clinical trials [22]. We have now made progress due to a focused effort to obtain tissue for research and the establishment of new experimental

model systems. Recent studies have demonstrated that DIPG is molecularly distinct from not only adult but also pediatric supratentorial gliomas [1,34,35,43,49,55]. Moreover, a specific, recurrent mutation in histone 3 at lysine 27 (H3 K27M) affecting the H3F3A gene (histone 3.3) or the HIST1H3B (histone 3.1) gene is found in nearly 80% of DIPG tumors [23,43,49,53]. Thalamic high-grade gliomas of childhood share this specific recurrent K27M point mutation in histone 3.1 or 3.3 genes, while pediatric cortical high-grade glioma exhibit a similarly specific histone 3 mutation at a different site [43,49]. Elegant studies have demonstrated that the recurrent histone 3 K27M mutation results in global loss of function of EZH2, a critical component of the epigenetic machinery responsible for trimethylation of lysine 27 in the N terminal tail of the histone, along with broad changes in the epigenetic landscape [3,26]. Yet, further research is needed to fully understand how these epigenetic changes are linked to DIPG tumorigenesis. Strikingly, DIPG presents in a specific temporal window, peaking in incidence at 6–9 years old [30], and in a specific anatomical area (the ventral pons) [12]. Hence, not only its genetic composition but also the pontine microenvironment at mid-childhood may account for the aggressive growth pattern and resistance to therapy this cancer exhibits.

Given the urgent need for translational studies on DIPG, we set out to develop models for this disease using *post mortem* DIPG tissue [7,30]. The direct method was attempted to avoid loss of putative important microenvironment growth factors after *in vitro* culture [31,48]; the indirect method was used to allow DIPG cell expansion. Interestingly, all tumors developed in the murine pons, and only in one case in the striatum, but in none subcutaneously. This observation may provide further evidences of the importance of the brain and particularly of the pontine microenvironment in facilitating DIPG tumor growth. At two independent institutions, all tumors developed after direct injection of DIPG cells (without *in vitro* expansion) proved to be of murine and not of human origin, signifying that human DIPG cells, via mechanisms still to be elucidated, induced transformation of healthy murine brain cells into malignant ones. Conversely, h-SU-DIPG-VI cells, expanded *in vitro* before *in vivo* xenotransplantation, gave rise to tumors of human origin. To prove that the indirect method consistently allows development of human DIPG xenografts, the direct and indirect methods need to be tested in parallel on the same *post mortem* DIPG cells. Of note, although we performed different control experiments with *post mortem* tissue not affected by brain cancer, we cannot exclude that development of murine tumors could also occur after injection of other glioma or other non-brain cancer cells. While h-SU-DIPG-VI cells resulted negative for the H-2K^{d}, a murine marker, not all murine neoplastic cells resulted positive; it has been reported that H-2K^{d} is absent in murine neural stem cells [20,28].

Clearly, these findings raise multiple mechanistic questions. Although not yet described for DIPG tumors, the occurrence of mouse tumors after injection of human tumor cells has been previously reported as a sporadic event [2,15,17,18,41,45,46,51], and may be attributable to viral transformation [2], human growth factor stimulation [50], cell fusion [13,14,16,17] or transference of human DNA into the mouse host cells [18]. Such events may lead to single catastrophic events causing the rapid and reproducible onset of mouse DIPG tumors as observed here [47]. It is unique to this study that, in all cases attempted with the direct xenotransplantation method, a murine and not a human tumor developed [9,11,27,33,36].

Different reports have demonstrated the presence of human DNA [18] and even human protein expression [17] in cancer cells with the genetic background of the host species [32]. In our studies we did not find any evidence of human genes or proteins in the murine neoplasms, possibly due to limitations of the methods employed. Thus, alternative approaches, such as whole genome sequencing, and analysis of the original xenografts, that developed directly after human cell injection, are warranted. A previous study, in which human GBM cells induced transformation of host hamster cells, reported that human chromosomes were segregated within the first transplant generation [17].

Finally, the murine neoplasm exhibited microglia/macrophage markers, as did approximately 20% of the h-SU-DIPG-VI cells. Hence, we analyzed *post mortem* DIPG tissue and identified microglia/macrophages in the tumor parenchyma. Although there are no reports yet evaluating these cell types in the DIPG microenvironment, studies have shown that cells expressing microglia/macrophage markers comprise 30–50% of the cells in benign and malignant gliomas [40]. While the role of microglia/macrophages in glioma has been controversial [52], recent studies have demonstrated that pharmacologic and genetic inhibition of microglial/macrophage function reduces tumor growth in experimental rodent glioma models [25,29,37] and the inhibition of colony stimulating factor-1 receptor has been shown to block glioma progression in a transgenic mouse model of proneuronal GBM [39]. Intriguingly, it has been hypothesized that microglia/macrophages in the glioma microenvironment may be malignant cells themselves and, given their amoeboid properties, maybe capable of invading the surrounding parenchyma giving rise to tumor growth and even tumor metastasis [21].

In conclusion, this study highlights the need for diligent precaution when employing DIPG orthotopic xenograft models, and possibly other glioma and non-brain tumor models, to exclude a murine origin of the resulting tumor. It is tempting to speculate that this phenomenon may underscore a biological process relevant to the human disease; alternatively this may be a phenomenon attributable to the altered immune function of the recipient immunodeficient mouse. The work presented here represents an important consideration for orthotopic xenograft models of DIPG, requiring careful species analysis to ensure that preclinical testing is performed in models as faithful to the human disease as possible.

Supplementary Material

Refer to Web version on PubMed Central for supplementary material.

Acknowledgments

We would like to thank the patients and families who so generously donated tissue for this research. We sincerely thank architect and artist Alessandra Luoni for drawing Fig. 1a. We gracefully acknowledge Alyssa Noll (Departments of Neurology and Pediatrics) for precious support with animal experiments, and Patty Lovelace (FACS Core) for her expertise with flow cytometry experiments; all from Stanford, United States. The flow cytometer used was purchased using a NIH S10 Shared Instrumentation Grant (1S10RR02933801). We are thankful to Jacqueline Cloos (Department of Pediatric Oncology, VU University Medical Center, The Netherlands) and Dana Bangs (Cytogenetics Laboratory, Stanford, United States) for their mastery in analyzing metaphase spreads. We are also thankful to Sridevi Yadavilli for processing *post mortem* specimens and assisting in murine injections, Research Center for Genetic Medicine, Children's National Medical Center, Washington, United States.

Funding

This work was supported by the Semmy Foundation, KiKa Children Cancer Free, Child Health Research Institute, Lucile Packard Foundation for Children's Health, as well as the Stanford CTSA -award number UL1 TR000093- (V.C.), Stanford University School of Medicine Dean's Fellowship (V.C.), National Institutes of Neurological Disease and Stroke (NINDS grant K08NS070926), Alex's Lemonade Stand Foundation, McKenna Claire Foundation, The Cure Starts Now, Lyla Nsouli Foundation, Connor Johnson Memorial Fund, Dylan Jewett Memorial Fund, Dylan Frick Memorial Fund, Abigail Jensen Memorial Fund, Zoey Ganesh Memorial Fund, Wayland Villars Memorial Fund and Musella Foundation.

References

1. Barrow J, Adamowicz-Brice M, Cartmill M, MacArthur D, Lowe J, Robson K, Brundler M, Walker DA, Coyle B, Grundy R. Homozygous loss of ADAM3A revealed by genome-wide analysis of pediatric high-grade glioma and diffuse intrinsic pontine gliomas. Neuro Oncol. 2011; 13:212–222. [PubMed: 21138945]
2. Beattie GM, Knowles AF, Jensen FC, Baird SM, Kaplan NO. Induction of sarcomas in athymic mice. Proc Natl Acad Sci U S A. 1982; 79:3033–3036. [PubMed: 6283553]
3. Bender S, Tang Y, Lindroth AM, Hovestadt V, Jones DTW, Kool M, Zapatka M, Northcott PA, Sturm D, Wang W, Radlwimmer B, Højfeldt JW, Truffaux N, Castel D, Schubert S, Ryzhova M, Seker-Cin H, Gronych J, Johann PD, Stark S, Meyer J, Milde T, Schuhmann M, Ebinger M, Monoranu C, Ponnuswami A, Chen S, Jones C, Witt O, Collins VP, von Deimling A, Jabado N, Puget S, Grill J, Helin K, Korshunov A, Lichter P, Monje M, Plass C, Cho Y, Pfister SM. Reduced H3K27me3 and DNA Hypomethylation Are Major Drivers of Gene Expression in K27M Mutant Pediatric High-Grade Gliomas. Cancer Cell. 2013; 24:660–72. [PubMed: 24183680]
4. Bugiani M, Boor I, van Kollenburg B, Postma N, Polder E, van Berkel C, van Kesteren RE, Windrem MS, Hol EM, Scheper GC, Goldman SA, van der Knaap MS. Defective glial maturation in vanishing white matter disease. J Neuropathol Exp Neurol. 2011; 70:69–82. [PubMed: 21157376]
5. Carertti, V.; Bugiani, M.; Boor, I.; Schellen, P.; Vandertop, WP.; Noske, DP.; Kaspers, GL.; Wurdinger, T.; Wesseling, P. Histopathological Heterogeneity in Diffuse Intrinsic Pontine Glioma. 15th International Symposium on Pediatric Neuro-Oncology; 2012.
6. Caretti, V. Pioneering preclinical research in diffuse intrinsic pontine glioma: towards new treatment strategies. Ipskamp Drukkers; Amsterdam: 2012.
7. Caretti V, Jansen MHA, van Vuurden DG, Lagerweij T, Bugiani M, Horsman I, Wessels H, van der Valk P, Cloos J, Noske DP, Vandertop WP, Wesseling P, Wurdinger T, Hulleman E, Kaspers GJL. Implementation of a Multi-Institutional Diffuse Intrinsic Pontine Glioma Autopsy Protocol and Characterization of a Primary Cell Culture. Neuropathol Appl Neurobiol. 2012; 39:426–36. [PubMed: 22845849]
8. Caretti V, Zondervan I, Meijer DH, Idema S, Vos W, Hamans B, Bugiani M, Hulleman E, Wesseling P, Vandertop WP, Noske DP, Kaspers G, Molthoff CFM, Wurdinger T. Monitoring of tumor growth and post-irradiation recurrence in a diffuse intrinsic pontine glioma mouse model. Brain Pathol. 2011; 21:441–451. [PubMed: 21159008]
9. Chen EH, Olson EN. Unveiling the mechanisms of cell-cell fusion. Science. 2005; 308:369–373. [PubMed: 15831748]
10. Donaldson SS, Laningham F, Fisher PG. Advances toward an understanding of brainstem gliomas. J Clin Oncol. 2006; 24:1266–1272. [PubMed: 16525181]
11. Duelli D, Lazebnik Y. Cell-to-cell fusion as a link between viruses and cancer. Nat Rev Cancer. 2007; 7:968–976. [PubMed: 18034186]
12. Fisher PG, Breiter SN, Carson BS, Wharam MD, Williams JA, Weingart JD, Foer DR, Goldthwaite PT, Tihan T, Burger PC. A clinicopathologic reappraisal of brain stem tumor classification. Identification of pilocystic astrocytoma and fibrillary astrocytoma as distinct entities. Cancer. 2000; 89:1569–1576. [PubMed: 11013373]
13. Goldenberg DM, Bhan RD, Pavia RA. In vivo human-hamster somatic cell fusion indicated by glucose 6-phosphate dehydrogenase and lactate dehydrogenase profiles. Cancer Res. 1971; 31:1148–1152. [PubMed: 5095979]

14. Goldenberg DM, Gold DV, Loo M, Liu D, Chang C, Jaffe ES. Horizontal transmission of malignancy: in-vivo fusion of human lymphomas with hamster stroma produces tumors retaining human genes and lymphoid pathology. PLoS One. 2013; 8:e55324. [PubMed: 23405135]
15. Goldenberg DM, Pavia RA. Malignant potential of murine stromal cells after transplantation of human tumors into nude mice. Science. 1981; 212:65–67. [PubMed: 7209521]
16. Goldenberg DM, Pavia RA, Tsao MC. In vivo hybridisation of human tumour and normal hamster cells. Nature. 1974; 250:649–651. [PubMed: 4859359]
17. Goldenberg DM, Zagzag D, Heselmeyer-Haddad KM, Berroa Garcia LY, Ried T, Loo M, Chang C, Gold DV. Horizontal transmission and retention of malignancy, as well as functional human genes, after spontaneous fusion of human glioblastoma and hamster host cells In Vivo. Int J Cancer. 2011; 131:49–58. [PubMed: 21796629]
18. Gupta V, Rajaraman S, Gadson P, Costanzi JJ. Primary transfection as a mechanism for transformation of host cells by human tumor cells implanted in nude mice. Cancer Res. 1987; 47:5194–5201. [PubMed: 3621205]
19. Hargrave D, Bartels U, Bouffet E. Diffuse brainstem glioma in children: critical review of clinical trials. Lancet Oncol. 2006; 7:241–248. [PubMed: 16510333]
20. Hori J, Ng TF, Shatos M, Klassen H, Streilein JW, Young MJ. Neural progenitor cells lack immunogenicity and resist destruction as allografts. Stem Cells. 2003; 21:405–16. [PubMed: 12832694]
21. Huysentruyt LC, Akgoc Z, Seyfried TN. Hypothesis: are neoplastic macrophages/microglia present in glioblastoma multiforme? ASN Neuro. 2011:epii: e00064.
22. Jansen MHA, van Vuurden DG, Vandertop WP, Kaspers GJL. Diffuse intrinsic pontine gliomas: A systematic update on clinical trials and biology. Cancer Treat Rev. 2012; 38:27–35. [PubMed: 21764221]
23. Khuong-Quang D, Buczkowicz P, Rakopoulos P, Liu X, Fontebasso AM, Bouffet E, Bartels U, Albrecht S, Schwartzentruber J, Letourneau L, Bourgey M, Bourque G, Montpetit A, Bourret G, Lepage P, Fleming A, Lichter P, Kool M, von Deimling A, Sturm D, Korshunov A, Faury D, Jones DT, Majewski J, Pfister SM, Jabado N, Hawkins C. K27M mutation in histone H3.3 defines clinically and biologically distinct subgroups of pediatric diffuse intrinsic pontine gliomas. Acta Neuropathol. 2012; 124:439–47. [PubMed: 22661320]
24. Krijgsman O, Israeli D, Haan JC, van Essen HF, Smeets SJ, Eijk PP, Steenbergen MRD, Kok K, Tejpar S, Meijer GA, Ylstra B. CGH arrays compared for DNA isolated from formalin-fixed, paraffin-embedded material. Genes Chromosomes Cancer. 2012; 51:344–52. [PubMed: 22162309]
25. Levy A, Blacher E, Vaknine H, Lund FE, Stein R, Mayo L. CD38 deficiency in the tumor microenvironment attenuates glioma progression and modulates features of tumor-associated microglia/macrophages. Neuro Oncol. 2012; 14:1037–49. [PubMed: 22700727]
26. Lewis PW, Müller MM, Koletsky MS, Cordero F, Lin S, Banaszynski LA, Garcia BA, Muir TW, Becher OJ, Allis CD. Inhibition of PRC2 activity by a gain-of-function H3 mutation found in pediatric glioblastoma. Science. 2013; 340:857–61. [PubMed: 23539183]
27. Lu X, Kang Y. Efficient acquisition of dual metastasis organotropism to bone and lung through stable spontaneous fusion between MDA-MB-231 variants. Proc Natl Acad Sci U S A. 2009; 106:9385–9390. [PubMed: 19458257]
28. Mammolenti M, Gajavelli S, Tsoulfas P, Levy R. Absence of major histocompatibility complex class I on neural stem cells does not permit natural killer cell killing and prevents recognition by alloreactive cytotoxic T lymphocytes in vitro. Stem Cells. 2004; 22:1101–10. [PubMed: 15536199]
29. Markovic DS, Vinnakota K, van Rooijen N, Kiwit J, Synowitz M, Glass R, Kettenmann H. Minocycline reduces glioma expansion and invasion by attenuating microglial MT1-MMP expression. Brain Behav Immun. 2011; 25:624–8. [PubMed: 21324352]
30. Monje M, Mitra SS, Freret ME, Raveh TB, Kim J, Masek M, Attema JL, Li G, Haddix T, Edwards MSB, Fisher PG, Weissman IL, Rowitch DH, Vogel H, Wong AJ, Beachy PA. Hedgehog-responsive candidate cell of origin for diffuse intrinsic pontine glioma. Proc Natl Acad Sci U S A. 2011; 108:4453–4458. [PubMed: 21368213]

31. Naundorf H, Fichtner I, Elbe B, Saul GJ, Haensch W, Zschiesche W, Reinecke S. Establishment and characteristics of two new human mammary carcinoma lines in nude mice with special reference to the estradiol receptor status and the importance of stroma for in vivo and in vitro growth. Breast Cancer Res Treat. 1994; 32:187–196. [PubMed: 7865848]
32. Ogle BM, Butters KA, Plummer TB, Ring KR, Knudsen BE, Litzow MR, Cascalho M, Platt JL. Spontaneous fusion of cells between species yields trans differentiation and retroviral transfer in vivo. FASEB J. 2004; 18:548–550. [PubMed: 14715691]
33. Ogle BM, Cascalho M, Platt JL. Biological implications of cell fusion. Nat Rev Mol Cell Biol. 2005; 6:567–575. [PubMed: 15957005]
34. Paugh BS, Broniscer A, Qu C, Miller CP, Zhang J, Tatevossian RG, Olson JM, Geyer JR, Chi SN, da Silva NS, Onar-Thomas A, Baker JN, Gajjar A, Ellison DW, Baker SJ. Genome-Wide Analyses Identify Recurrent Amplifications of Receptor Tyrosine Kinases and Cell-Cycle Regulatory Genes in Diffuse Intrinsic Pontine Glioma. J Clin Oncol. 2011; 29:3999–4006. [PubMed: 21931021]
35. Paugh BS, Qu C, Jones C, Liu Z, Adamowicz-Brice M, Zhang J, Bax DA, Coyle B, Barrow J, Hargrave D, Lowe J, Gajjar A, Zhao W, Broniscer A, Ellison DW, Grundy RG, Baker SJ. Integrated Molecular Genetic Profiling of Pediatric High-Grade Gliomas Reveals Key Differences With the Adult Disease. J Clin Oncol. 2010; 28:3061–3068. [PubMed: 20479398]
36. Pawelek JM, Chakraborty AK. The cancer cell-leukocyte fusion theory of metastasis. Adv Cancer Res. 2008; 101:397–444. [PubMed: 19055949]
37. Pong WW, Higer SB, Gianino SM, Emnett RJ, Gutmann DH. Reduced microglial CX3CR1 expression delays neurofibromatosis-1 glioma formation. Ann Neurol. 2013; 73:303–8. [PubMed: 23424002]
38. Press CSHL. Fluorescence in situ hybridization. Nat Meth. 2005; 2:237–238.
39. Pyonteck SM, Akkari L, Schuhmacher AJ, Bowman RL, Sevenich L, Quail DF, Olson OC, Quick ML, Huse JT, Teijeiro V, Setty M, Leslie CS, Oei Y, Pedraza A, Zhang J, Brennan CW, Sutton JC, Holland EC, Daniel D, Joyce JA. CSF-1R inhibition alters macrophage polarization and blocks glioma progression. Nat Med. 2013; 19:1264–72. [PubMed: 24056773]
40. Roggendorf W, Strupp S, Paulus W. Distribution and characterization of microglia/macrophages in human brain tumors. Acta Neuropathol. 1996; 92:288–93. [PubMed: 8870831]
41. Russell PJ, Brown J, Grimmond S, Stapleton P, Russell P, Raghavan D, Symonds G. Tumour-induced host stromal-cell transformation: induction of mouse spindle-cell fibrosarcoma not mediated by gene transfer. Int J Cancer. 1990; 46:299–309. [PubMed: 2384276]
42. Saratsis AM, Kambhampati M, Snyder K, Yadavilli S, Devaney JM, Harmon B, Hall J, Raabe EH, An P, Weingart M, Rood BR, Magge SN, Macdonald TJ, Packer RJ, Nazarian J. Comparative multidimensional molecular analyses of pediatric diffuse intrinsic pontine glioma reveals distinct molecular subtypes. Acta Neuropathol. 2013
43. Schwartzentruber J, Korshunov A, Liu X, Jones DTW, Pfaff E, Jacob K, Sturm D, Fontebasso AM, Quang DK, Tönjes M, Hovestadt V, Albrecht S, Kool M, Nantel A, Konermann C, Lindroth A, Jäger N, Rausch T, Ryzhova M, Korbel JO, Hielscher T, Hauser P, Garami M, Klekner A, Bognar L, Ebinger M, Schuhmann MU, Scheurlen W, Pekrun A, Frühwald MC, Roggendorf W, Kramm C, Dürken M, Atkinson J, Lepage P, Montpetit A, Zakrzewska M, Zakrzewski K, Liberski PP, Dong Z, Siegel P, Kulozik AE, Zapatka M, Guha A, Malkin D, Felsberg J, Reifenberger G, von Deimling A, Ichimura K, Collins VP, Witt H, Milde T, Witt O, Zhang C, Castelo-Branco P, Lichter P, Faury D, Tabori U, Plass C, Majewski J, Pfister SM, Jabado N. Driver mutations in histone H3.3 and chromatin remodelling genes in paediatric glioblastoma. Nature. 2012; 482:226–31. [PubMed: 22286061]
44. Sethi R, Allen J, Donahue B, Karajannis M, Gardner S, Wisoff J, Kunnakkat S, Mathew J, Zagzag D, Newman K, Narayana A. Prospective neuraxis MRI surveillance reveals a high risk of leptomeningeal dissemination in diffuse intrinsic pontine glioma. J Neurooncol. 2010; 99:1–7. [PubMed: 20020177]
45. Soranzo C, Ingrosso A, Pratesi G, Lombardi L, Pilotti S, Zunino F. Malignant transformation of host cells by a human small cell lung cancer xenografted into nude mice. Anticancer Res. 1989; 9:361–366. [PubMed: 2546483]

46. Sparrow S, Jones M, Billington S, Stace B. The in vivo malignant transformation of mouse fibroblasts in the presence of human tumour xenografts. Br J Cancer. 1986; 53:793–797. [PubMed: 3013267]
47. Stephens PJ, Greenman CD, Fu B, Yang F, Bignell GR, Mudie LJ, Pleasance ED, Lau KW, Beare D, Stebbings LA, McLaren S, Lin M, McBride DJ, Varela I, Nik-Zainal S, Leroy C, Jia M, Menzies A, Butler AP, Teague JW, Quail MA, Burton J, Swerdlow H, Carter NP, Morsberger LA, Iacobuzio-Donahue C, Follows GA, Green AR, Flanagan AM, Stratton MR, Futreal PA, Campbell PJ. Massive genomic rearrangement acquired in a single catastrophic event during cancer development. Cell. 2011; 144:27–40. [PubMed: 21215367]
48. Stuelten CH, Busch JI, Tang B, Flanders KC, Oshima A, Sutton E, Karpova TS, Roberts AB, Wakefield LM, Niederhuber JE. Transient tumor-fibroblast interactions increase tumor cell malignancy by a TGF-Beta mediated mechanism in a mouse xenograft model of breast cancer. PLoS One. 2010; 5:e9832. [PubMed: 20352126]
49. Sturm D, Witt H, Hovestadt V, Khuong-Quang D, Jones DTW, Konermann C, Pfaff E, Tönjes M, Sill M, Bender S, Kool M, Zapatka M, Becker N, Zucknick M, Hielscher T, Liu X, Fontebasso AM, Ryzhova M, Albrecht S, Jacob K, Wolter M, Ebinger M, Schuhmann MU, van Meter T, Frühwald MC, Hauch H, Pekrun A, Radlwimmer B, Niehues T, von Komorowski G, Dürken M, Kulozik AE, Madden J, Donson A, Foreman NK, Drissi R, Fouladi M, Scheurlen W, von Deimling A, Monoranu C, Roggendorf W, Herold-Mende C, Unterberg A, Kramm CM, Felsberg J, Hartmann C, Wiestler B, Wick W, Milde T, Witt O, Lindroth AM, Schwartzentruber J, Faury D, Fleming A, Zakrzewska M, Liberski PP, Zakrzewski K, Hauser P, Garami M, Klekner A, Bognar L, Morrissy S, Cavalli F, Taylor MD, van Sluis P, Koster J, Versteeg R, Volckmann R, Mikkelsen T, Aldape K, Reifenberger G, Collins VP, Majewski J, Korshunov A, Lichter P, Plass C, Jabado N, Pfister SM. Hotspot mutations in H3F3A and IDH1 define distinct epigenetic and biological subgroups of glioblastoma. Cancer Cell. 2012; 22:425–37. [PubMed: 23079654]
50. Todaro GJ, Fryling C, De Larco JE. Transforming growth factors produced by certain human tumor cells: polypeptides that interact with epidermal growth factor receptors. Proc Natl Acad Sci U S A. 1980; 77:5258–5262. [PubMed: 6254071]
51. Wakasugi H, Koyama K, Gyotoku M, Yoshimoto M, Hirohashi S, Sugimura T, Terada M. Frequent development of murine T-cell lymphomas with TcR alpha/beta+, CD4-/8- phenotype after implantation of human inflammatory breast cancer cells in BALB/c nude mice. Jpn J Cancer Res. 1995; 86:1086–1096. [PubMed: 8567401]
52. Wei J, Gabrusiewicz K, Heimberger A. The controversial role of microglia in malignant gliomas. Clin Dev Immunol. 2013; 2013:285246. [PubMed: 23983766]
53. Wu G, Broniscer A, McEachron TA, Lu C, Paugh BS, Becksfort J, Qu C, Ding L, Huether R, Parker M, Zhang J, Gajjar A, Dyer MA, Mullighan CG, Gilbertson RJ, Mardis ER, Wilson RK, Downing JR, Ellison DW, Zhang J, Baker SJ. Somatic histone H3 alterations in pediatric diffuse intrinsic pontine gliomas and non-brainstem glioblastomas. Nat Genet. 2012; 44:251–253. [PubMed: 22286216]
54. Yoshimura J, Onda K, Tanaka R, Takahashi H. Clinicopathological study of diffuse type brainstem gliomas: analysis of 40 autopsy cases. Neurol Med Chir. 2003; 43:375–382.
55. Zarghooni M, Bartels U, Lee E, Buczkowicz P, Morrison A, Huang A, Bouffet E, Hawkins C. Whole-Genome Profiling of Pediatric Diffuse Intrinsic Pontine Gliomas Highlights Platelet-Derived Growth Factor Receptor alpha and Poly (ADP-ribose) Polymerase As Potential Therapeutic Targets. J Clin Oncol. 2010; 28:1337–1344. [PubMed: 20142589]

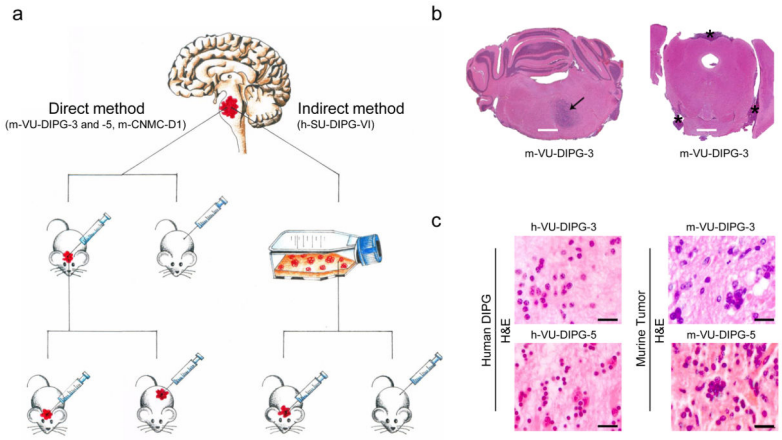

Fig. 1. Direct and indirect xenotransplantation of human post mortem DIPG cells gives rise to tumors resembling the original DIPG neuropathology

(a) Sketch summarizing the direct and indirect method adopted to develop DIPG xenograft mouse models. DIPG tumor tissue (symbolized in red) was obtained at autopsy. The direct method consisted of rapid mechanical dissociation and xenotransplantation, while the indirect method comprised an intermediate *in vitro* culturing step followed by *in vivo* injection. Using both methods, xenografts developed in the pons but not subcutaneously. In the direct method, xenografts were serially transplanted from the pons or striatum (only for m-VU-DIPG-3) of a mouse to the pons of another mouse and subcutaneously. Henceforth, the xenografts grew subcutaneously as well as in the pons. (b) Low H&E magnification image of m-VU-DIPG-3 xenograft at transplant generation 1 *in vivo*. Note the diffuse growth pattern in the ventral pons (arrow) and in the leptomeninges (asterisks). (c) H&E of small-cell DIPG phenotype in h-VU-DIPG-3 and -5 tissues and correspondent m-VU-DIPG-3 (transplant generation 1) and -5 (transplant generation 2) pontine tissue. Scale bars = (B) 1mm and (C) 20 μm.

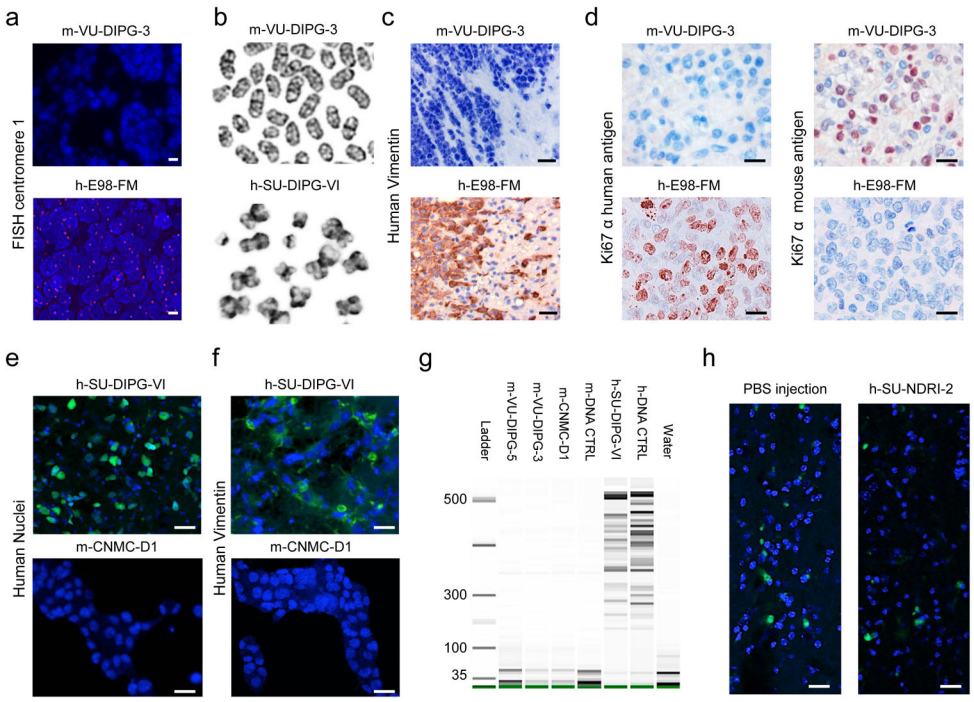

Fig. 2. Human DIPG cells injected directly from the human brain to the mouse brain induce lethal murine pontine tumors

Murine VU-DIPG-3 and -5 (transplant generation 1 and 2, respectively) and h-E98-FM pontine tumor tissues were subjected to (a) FISH for human centromere 1 (fuscia), (c) human Vimentin and (d) Ki67 immunostaining against the human and mouse antigen. (b) Metaphase spreads demonstrating the typical telocentric mouse karyotype in m-VU-DIPG-3 (transplant generations 3–10) and classical X shape of human chromosome in h-SU-DIPG-VI. Human-SU-DIPG-VI cells were cultured *in vitro* for 6 passages. (e and f) Human-SU-DIPG-VI pontine xenografts (h-SU-DIPG-VI cells passaged *in vitro* 6 times before xenotransplantation) and m-CNMC-D1 cells were stained for antibodies directed against (e) Human Nuclei antigen (green) and (f) human Vimentin (green). Murine CNMC-D1 cells were obtained form pontine xenograft (transplant generation 1) and passaged *in vitro* 5 times. (g) DNA fingerprinting showing no overlap between h-SU-DIPG-VI and h-DNA-CTRL and m-VU-DIPG-3 and-5, m-CNMC-D1 and m-DNA-CTRL bands, indicating that no significant human STR is found in any of the murine tumor samples. DNA was extracted from cells obtained at transplant generations 3–10 (m-VU-DIPG-3 and -5) and 1 (m-CNMC-D1 cells were then cultured *in vitro* for 6 passages). (h) PBS or a single cells suspension, derived from *post mortem* human pontine tissue not affected by brain cancer, was injected in the murine pons. The only cells positive for Ki67 staining (green) were detected in the proximity of the needle trajectory, indicating response to tissue damage. No tumor formation could be detected. (a, e, f, h) Blue = DAPI. (c and d) Blue= hematoxylin. Scale bars = (a) 5 μm; (c, e, f and h) 20 μm; (d) 10μm.

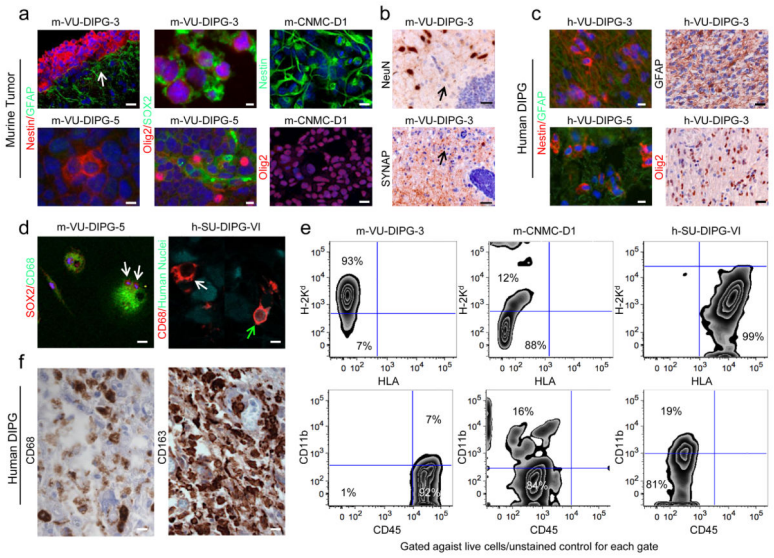

Fig. 3. Murine pontine tumors exhibit neural markers and microglial markers

(a) Immunohistochemical analysis of PPC markers, Nestin (red and green for m-CNMC-D1), Olig2 (red), SOX2 (green) and GFAP (green) for m-VU-DIPG-3 and -5 pontine tumors and m-CNMC-D1 cells. Murine-VU-DIPG-3 and -5 images refer to transplant generation 1 and 2, respectively, while m-CNMC-D1 cells were obtained form pontine xenograft (transplant generation 1) and cultured *in vitro* for 5 passages. The arrow indicates reactive gliosis comprised of $GFAP^+$ host cells surrounding the tumor. (c) As in (a) for the original h-VU-DIPG-3 and -5 tumor (b) Murine VU-DIPG-3 and -5 pontine xenografts (transplant generations 3–10) are negative for the neuronal markers NeuN and synaptophysin (SYNAP), in contrast to host neurons (upper panel) and the neuropil rich in synapses (lower panel). Arrows indicate the diffuse component of the tumors. (d) Murine-VU-DIPG-5 cells obtained from subcutaneous tumors (transplant generations 3–10) and cultured on chamber slides resulted positive for CD68 (green) and SOX2 (red). Note the presence of multinucleated cells (arrows). Human SU-DIPG-VI xenograft (h-SU-DIPG-VI cells passaged *in vitro* 6 times before xenotransplantation) exhibit sparsely distributed cells immunopositive both for the Human Nuclei antigen (green) and for CD68 (red) (green arrow). Note the presence of a CD68 positive cell that is not positive for Human Nuclei antigen (white arrow) (e) Flow cytometry analysis for $H\text{-}2K^d$, HLA, CD45 and CD11b. On the y- and x-axes the logarithmic intensity of the fluorophore is depicted. Murine-VU-DIPG-3 cells were obtained from subcutaneous tumors (transplant generations 3–10); m-CNMC-D1 cells were obtained form pontine xenograft (transplant generation 1) and cultured *in vitro* for 8 passages and h-SU-DIPG-VI were cultured *in vitro* for 12 passages. (f) Human-SU-DIPG-I *post mortem* pontine tissue is immunopositive for CD68 and CD163 microglia/macrophage markers. (a, c, left panels and d) Blue = DAPI. (c, right panels and f) Blue= hematoxylin. Scale bars = (a, left panels) m-VU-DIPG-3 50 μm and m-VU-DIPG-5 10 μm; (a, central and right panels and c) m-VU-DIPG-3 10 μm, m-VU-DIPG-5 and m-CNMC-D1 20 μm; (b) m-VU-DIPG-3 12.5 μm and m-VU-DIPG-5 25 μm; (d, left panel and f) 10 μm and (d, right panel) 5 μm.

Table 1

Patients' clinical characteristics

This table summarizes the clinical characteristics of patients whose DIPG *post mortem* tissue was employed to develop DIPG models via the direct and indirect methods. WHO refers to World Health Organization and GBM refers to glioblastoma multiforme (WHO grade IV).

	Direct Method				Indirect Method
Patient	**h-VU-DIPG-3**	**h-VU-DIPG-4**	**h-VU-DIPG-5**	**h-CNMC-D1**	**h-SU-DIPG-VI**
Age (years)	1	7.5	7	21	7
Sex	F	M	M	M	F
Survival time (months)	11	5	20	19	6
Time to Progression (months)	3	3	12	4	5
Death-Autopsy Interval (hours)	3.5	4	3	3	2
H3F3A K27M status	+	+	+	−	+
Histological diagnosis at autopsy	GBM	GBM	GBM	GBM	Astrocytoma (WHO grade III)

Table 2

Genetic characterization of VU-DIPG-3 and -5 human tumors and murine xenografts

DNA from m-VU-DIPG-3 and -5 was isolated from subcutaneous tumor at transplant generation 1 and 2, respectively. n.a.: not analyzable.

	VU-DIPG-3		VU-DIPG-5	
	human	**murine**	**human**	**murine**
Specific mutation				
H3F3A K27M	+	−	+	−
H3F3A G34R	−	−	−	−
HIST1H3B K27M	−	−	−	−
PI3KCA H1047R	−	−	−	−
PI3KCA H1047L	−	−	−	−
PI3KCA E542K	−	−	−	−
Amplification				
EGFR	−	−	n.a.	n.a.
PTEN	−	−	Deletion	n.a.
PDGFR-α	−	−	n.a.	n.a.
Array CGH profile				
Human 180K	Gain 1q, loss 17p (distal)	n.a.	n.a.	n.a.
Mouse 180K	n.a.	Loss 4 (C4-C5), gain 4 (C5-D2.2)	n.a.	n.a.